Citation: Molecular Therapy—Nucleic Acids (2015) 4, e267; doi:10.1038/mtna.2015.41
Official journal of the American Society of Gene & Cell Therapy

www.nature.com/mtna

Electroporation Enhanced Effect of Dystrophin Splice Switching PNA Oligomers in Normal and Dystrophic Muscle

Camilla Brolin[1,2], Takehiko Shiraishi[2], Pernille Hojman[4], Thomas O Krag[5], Peter E Nielsen[2,3] and Julie Gehl[1]

Peptide nucleic acid (PNA) is a synthetic DNA mimic that has shown potential for discovery of novel splice switching antisense drugs. However, *in vivo* cellular delivery has been a limiting factor for development, and only few successful studies have been reported. As a possible modality for improvement of *in vivo* cellular availability, we have investigated the effect of electrotransfer upon intramuscular (i.m.) PNA administration *in vivo*. Antisense PNA targeting exon 23 of the murine dystrophin gene was administered by i.m. injection to the tibialis anterior (TA) muscle of normal NMRI and dystrophic mdx mice with or without electroporation. At low, single PNA doses (1.5, 3, or 10 µg/TA), electroporation augmented the antisense exon skipping induced by an unmodified PNA by twofold to fourfold in healthy mouse muscle with optimized electric parameters, measured after 7 days. The PNA splice switching was detected at the RNA level up to 4 weeks after a single-dose treatment. In dystrophic muscles of the MDX mouse, electroporation increased the number of dystrophin-positive fibers about 2.5-fold at 2 weeks after a single PNA administration compared to injection only. In conclusion, we find that electroporation can enhance PNA antisense effects in muscle tissue.

Molecular Therapy—Nucleic Acids (2015) **4**, e267; doi:10.1038/mtna.2015.41; published online 1 December 2015
Subject Category: Nucleic acid chemistries

Introduction

PNA is an artificial DNA mimic with possible application in antisense drug discovery, *e.g.*, as splice switching agents designed to sterically block splice sites or specific binding motifs for the splicing machinery, resulting in exon skipping.[1] However, exploitation of the full potential of PNA as antisense agents is currently limited by poor pharmacokinetics (t½ ~ ½ hour) and cellular uptake of unmodified PNA.[2,3] Several delivery methods have been explored to enhance *in vitro* cellular uptake, including micro injection, electroporation, PNA liposome formulations, conjugation of PNA to cell-penetrating peptides or to receptor-targeted ligands,[1,4] and *in vivo* activity using PNA conjugates has been demonstrated.[3,5] However, efficiency has so far been very low, presumably due to a combination of nonoptimal pharmacokinetics and poor cellular uptake in target tissues.

Electroporation has successfully been employed to enhance both cellular and *in vivo* delivery of therapeutically interesting agents ranging from low-molecular-weight anticancer drugs to large DNA vectors and has also yielded impressive clinical results in local cancer treatment. For instance, electroporation in combination with chemotherapy is routinely used in the clinic for treatment of cutaneous metastasis (electrochemotherapy).[6,7] Furthermore, the field of electroporation-based therapies is rapidly expanding into targeting a range of different tissues such as internal tumors using newly developed electrodes[8,9] and also including a clinical phase 1 study investigating intramuscular (i.m.) electrotransfer of DNA (ClinicalTrials.gov: NCT01664273).

During the application of an external electric field across a tissue, a transient and reversible structural change at the level of the cell membrane is induced, leading to transient permeabilization of the cell, technically known as electroporation. During this state of permeabilization, cells can be loaded with small molecules through simple diffusion[10,11] or larger anionic molecules such as DNA, which may be electrophoretically driven into the cells.[12,13] The size of the molecule, as well as its charge, will significantly influence the efficiency and the mechanism of electrotransfer. Indeed, a recent study showed that not only the charge of PNA but also the electroporation method influenced the efficiency of PNA delivery to cells in culture.[14] Thus, in a cell suspension (using cuvettes), positively charged PNAs were more efficiently transferred, whereas charge neutral PNAs were more efficiently transferred in a microtiter plate electrotransfer system for surface-attached cells.[14]

Duchenne muscular dystrophy (DMD), the most common and severe form of muscular dystrophy, is caused by mutations in the dystrophin gene, reducing or abolishing the synthesis of functional dystrophin protein. Dystrophin is an essential, structural muscle protein that links the contractile elements to the extracellular matrix, thereby mediating force transmission from the sub-sarcolemmal actin to the extracellular matrix. Antisense-mediated exon skipping is so far one

[1]Center for Experimental Drug and Gene Electrotransfer (CEDGE), Department of Oncology, Copenhagen University Hospital Herlev, Denmark; [2]Department of Cellular and Molecular Medicine, Faculty of Health and Medical Sciences, The Panum Institute, University of Copenhagen, Denmark; [3]Department of Drug Design and Pharmacology, Faculty of Health and Medical Sciences, The Panum Institute, University of Copenhagen, Denmark; [4]The Centre of Inflammation and Metabolism and the Centre for Physical Activity Research, Department of Infectious Diseases, Rigshospitalet, University of Copenhagen, Denmark; [5]Neuromuscular Research Unit, Department of Neurology Rigshospitalet, University of Copenhagen, Denmark. Correspondence: Julie Gehl, Department of Oncology, Copenhagen University Hospital Herlev, Herlev Ringvej 75, DK-2730 Herlev, Denmark. E-mail: Karen.Julie.Gehl@regionh.dk or Peter E. Nielsen, Department of Cellular and Molecular Medicine, Faculty of Health and Medical Sciences, University of Copenhagen, Blegdamsvej 3C, DK-2200 Copenhagen N, Denmark. Email: ptrn@sund.ku.dk
Keywords: antisense; electroporation; exon skipping; mdx; PNA; splicing modulation
Received 29 June 2015; accepted 9 October 2015; advance online publication 1 December 2015. doi:10.1038/mtna.2015.41

of the most promising therapeutic approaches for DMD. Modulation of dystrophin pre-mRNA splicing by an antisense oligonucleotide can induce the formation of a partly functional dystrophin protein with intact N- and C-terminal ends but with a truncated rod-domain, capable of converting a DMD to the milder Becker muscular dystrophy phenotype.[15] Currently, two drugs, drisapersen (a 2′O-methyl phosphorothioate oligonucleotide) and eteplirsen (a morpholino oligomer), exploiting antisense induced DMD exon 51 skipping are in clinical trials for treatment of DMD. In both trials, production of dystrophin protein upon i.m. administration was demonstrated in phase 1 studies,[16,17] and for drisapersen, significant benefit in the 6-minute walking distance test compared to placebo was also reported.[18] However, the phase 3 drisapersen trial (with 186 patients) failed to meet the primary endpoint of statistically significant improvement in the 6-minute walking distance test compared to placebo.[19] In the phase 2b eteplirsen trial, an eightfold higher dose (up to 50 mg/kg) was used compared to drisapersen (6 mg/kg), and benefit of 67 m less decline in the 6-minute walking distance test in 12 patients compared to the placebo group was reported.[20]

In this study, we have investigated electrotransfer-facilitated i.m. administration of anti-dystrophin PNA to muscle tissue *in vivo*, using a PNA that was previously reported to induce exon 23 dystrophin mRNA skipping[21,22] and partial dystrophin protein restoration in dystrophic (mdx) mice.

Results

Optimization of pulse parameters and injection volume in NMRI mice

Short, high-voltage pulses (HV; ~1,000 V/cm, µs duration) are generally favored for electrotransfer of small molecules such as standard chemotherapeutics to tumors, while long, low-voltage pulses (LV; ~<250 V/cm, ms duration) have been used extensively for electrotransfer of vector DNA and other negatively charged molecules to muscles.[23–26] In order to optimize electric parameters for PNA electrotransfer in tibialis anterior (TA) muscles, we tested both HV and LV pulses, as well as a combination of these. PNA effect was measured by the degree of exon skipping in the muscle 7 days after treatment. An effect increase was observed using 8 HV pulses at 600 and 800 V/cm, (100 µs, 1 HZ) ($P < 0.01$ and $P < 0.05$, compared to injection only), while no significant effect increase of electroporation at 8 pulses of 1,000 V/cm (100 µs, 1 HZ) was found (**Figure 1a**). Higher exon skipping levels were observed after applying longer (20 ms) LV pulses compared to HV pulses. For instance, 175 and 200 V/cm improved exon skipping 3.8- and 4.2-fold, respectively ($P < 0.01$ and $P < 0.001$). On the other hand, a combination of a short HV and a longer LV pulse, which have been shown to mediate efficient vector DNA delivery,[27] had no effect on PNA efficacy. For further evaluation of the effect of LV ms pulses on PNA activity, electroporation with 8 pulses of 20 ms ranging from 125 to 250 V/cm at 1 Hz was performed. The results confirmed that the highest effect was obtained using eight 20-ms pulses above 175 V/cm at 1 Hz ($P < 0.05$ for 175, 200, and 250 V/cm) (**Figure 1b**).

In most antisense oligonucleotide exon skipping studies in TA mice muscle, an injection volume of 25–40 µl in the muscle has been used,[21,26] which corresponds to more than one-third of the muscle volume. This large volume is not clinically relevant and may result in uptake facilitated by the hydrostatic pressure from the injection. However, an increased transgene expression has been reported with low injection volumes.[28,29] Thus, we decided to study the effect of injection volume with a fixed dose (3 µg PNA/TA). Increasing the injection volume from 10 µl to 20 and 40 µl reduced the antisense effect with statistical significance (two-way analysis of variance (ANOVA) effect of volume, $P < 0.01$), and a statistically significant overall enhancement by electroporation was also found in this experiment (two-way ANOVA, effect of electroporation, $P < 0.05$) (**Figure 2**). Based on these results, an injection volume of 10 µl was considered most optimal.

Dose response and duration in NMRI mice

We next examined the dose dependency and duration of PNA-mediated exon skipping after i.m. administration. ANOVA of all data (**Figure 3a**) showed a clear dose response (two-way ANOVA, effect of dose, $P < 0.001$), and although electroporation yielded essential identical response at all doses, an overall electroporation enhancement was significant (two-way ANOVA, effect of electroporation, $P < 0.01$). In addition, the *post hoc* test showed statistical significance between muscles injected and electroporated with the 10 µg PNA dose ($P < 0.01$) (**Figure 3a**). In a second experiment, we administered increasing PNA doses in proportionally increasing volumes, and also under these conditions, statistically significant effect of dose as well as of electroporation was observed (two-way ANOVA, effect of dose, $P < 0.0001$ and two-way ANOVA, effect of electroporation, $P < 0.001$) (**Supplementary Figure S1**).

In order to determine the duration of the PNA effect, muscles were subjected to RT-PCR at 1, 2, 4, and 8 weeks after treatment with 10 µg PNA. In the absence of electroporation, the highest degree of exon skipping was seen at 2 weeks ($P < 0.05$), and hardly any exon skipping could be detected at 8 weeks. Also, in this experiment, electroporation increased exon skipping levels (two-way ANOVA, effect of electroporation, $P < 0.001$). This enhancement was most significant at week 1 (threefold; $P < 0.0001$) and week 4 ($P < 0.05$), and a yield exceeding 15% exon skipping was observed (**Figure 3b**). An approximately twofold increase in exon skipping percentage ($P < 0.05$) was seen at 2 weeks when compared to the 1-week time point after treatment without electroporation. Since the half-life of the dystrophin mRNA is around 16 hours[30] and the half-life of dystrophin protein is 2–4 months,[31,32] these results indicate that the PNA slowly accumulates in the muscle cells over 2 weeks and retains activity in the muscles for more than 4 weeks.

Electrotransfer of PNA conjugates

In vitro data on cultured cells have shown that the efficiency of electrotransfer is very significantly influenced by different delivery (peptide) ligands conjugated to the PNA.[14] In order to determine whether this is also the case concerning muscle delivery *in vivo*, a series of PNA-peptide conjugates was studied (**Table 1**), including two cationic octaarginine conjugates (PNA3687 and 3690),[33] a highly negatively charged

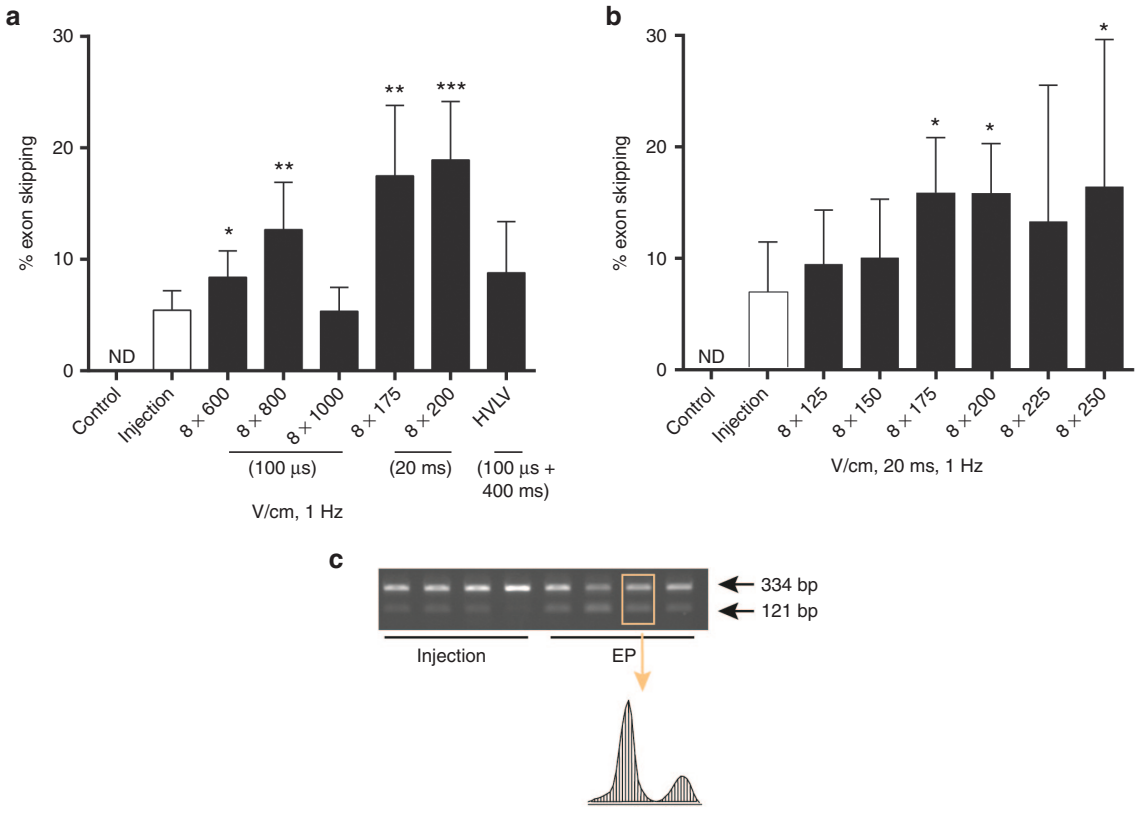

Figure 1 Optimization of electric pulse parameters in NMRI mice. Effect of electric pulses on PNA activity (measured by RT-PCR as exon skipping percentage) in TA muscle in NMRI mice using 3 µg/TA. Results are presented as mean + SD, injection only (white bars), electroporation (black bars), control = untreated, not detectable (ND). (**a**) The pulse parameters were: 8 pulses of (100 µs, 1 Hz, of varying V/cm), (175 V/cm and 200 V/cm, 1 Hz, 20 ms), and (HVLV= 1×800 V/cm, 100 µs + 1×80 V/cm, 400 ms), *t*-test (comparison of injection only and electroporation): **P* < 0.05; ***P* < 0.01; ****P* < 0.001 (*n* = 4–6). (**b**) Effect of ms pulses on PNA activity. One-way ANOVA followed by Dunnetts multiple comparison test; **P* < 0.05 (*n* = 4–12). (**c**) Examples of RT-PCR analysis of exon 23 skipping (121 bp) after PNA electrotransfer. Four representative samples from injection-only and electroporation (8×250 V/cm, 20 ms, 1 Hz) are shown, as well as an example of a corresponding densitometric scan from which the quantification of full-length and skipped DNA fragments was performed. Sequence analysis of the PCR product confirmed the precise exicision of exon 23 between exon 22 and 24 (data not shown). ANOVA, analysis of variance; PNA, peptide nucleic acid; TA, tibialis anterior.

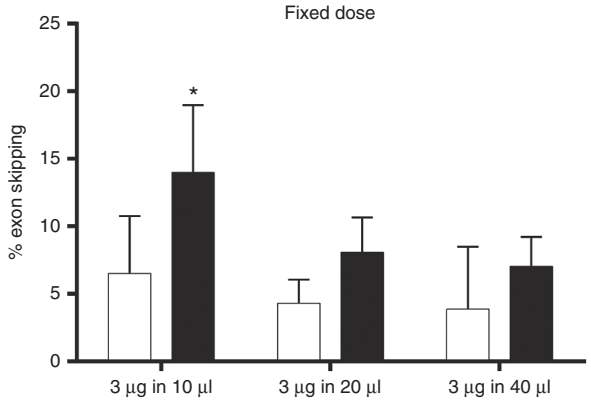

Figure 2 Optimization of injection volume in NMRI mice. Effect of electroporation on PNA activity using increasing injection volumes with a fixed dose (3 µg/TA) in TA muscles (*n* = 4–6). Results are presented as mean + SD (white bars = injection, black = electroporation). Electroporation parameters: (8×175 V/cm, 20 ms, 1 Hz). Two-way ANOVA followed by Tukey multiple comparison test: **P* < 0.05. ANOVA, analysis of variance; PNA, peptide nucleic acid; TA, tibialis anterior.

octaphosphonate conjugate (PNA 3684)[34] (which like oligonucleotides are efficiently delivered to cells via lipofection), and a tetralysine conjugate (PNA 4258) of which analogous conjugates targeting an engineered GFP gene have exhibited good *in vivo* exon 23 skipping activity upon systemic administration in a GFP mouse model.[3] Exon skipping activity was only observed with the unmodified PNA 3696, the octaarginine (PNA 3690) and tetralysine (PNA 4258) conjugates. ANOVA showed an overall effect of electroporation (two-way ANOVA, effect of electroporation, $P < 0.0001$), which in the *post hoc* test was statistically significant for the unmodified PNA 3696 ($P < 0.0001$), although a small increase in exon skipping was also seen for the tetralysine conjugate (**Figure 4**). Finally, as a control for antisense sequence specificity, a mismatch control PNA was tested at the same concentration (10 µg PNA), and no detectable exon skipping was observed (**Figure 4**).

PNA electrotransfer in muscles of mdx mice

Based on the optimization studies in NMRI mice, we chose to use an injection volume of 10 µl of unmodified PNA, electroporated using 8 LV pulses, 20 ms at 175 V/cm for further

studies in dystrophic mdx mice. In contrast to the results from the NMRI mice, electroporation did not increase the PNA effect measured in the muscles at the RNA level 1 week after treatment at low dose (3 µg) (**Figure 5** and **Supplementary Figure S2a**), whereas an enhancement, although not statistically significant, was indicated at the high doses (10 and 30 µg), compared to simple injection (**Figure 5a**). In mdx mice, which are lacking dystrophin protein, exon skipping can be detected both at the mRNA level as well as by immunostaining of the resulting new synthesis of partially intact dystrophin protein. Immunohistochemistry was performed at three positions along the muscle for analysis of the appearance of dystrophin-positive fibers. Whole muscle transverse sections showed recovery of dystrophin at the sarcolemma in PNA-injected regions in all three positions tested, whereas only few revertant fibers were observed in the untreated control muscles (**Figure 5b**). Quantification of the number of dystrophin-positive fibers per section showed PNA dose dependency (two-way ANOVA, effect of dose, $P < 0.0001$), and an overall enhancing effect of electroporation seen (two-way ANOVA, effect of electroporation, $P < 0.01$) (**Figure 5c**). The number of dystrophin-positive fibers reached more than 1,000 in some of the samples treated with 10 and 30 µg PNA, and the number of dystrophin-positive fibers was higher in the proximal sections (two-way ANOVA, effect of location, $P < 0.0001$). A parallel western blotting analysis qualitatively corroborated the conclusions from the immunostaining that dystrophin protein synthesis was indicated by the PNA treatment, but we did not attempt to quantify these data in the PNA-treated muscles (**Figure 5c**). Finally, RT-PCR determination of dystrophin mRNA splice redirection level in the whole muscle very nicely paralleled the total number of dystophin-positive fibers per muscle (compare results in **Figure 5a** and **Supplementary Figure S2b**).

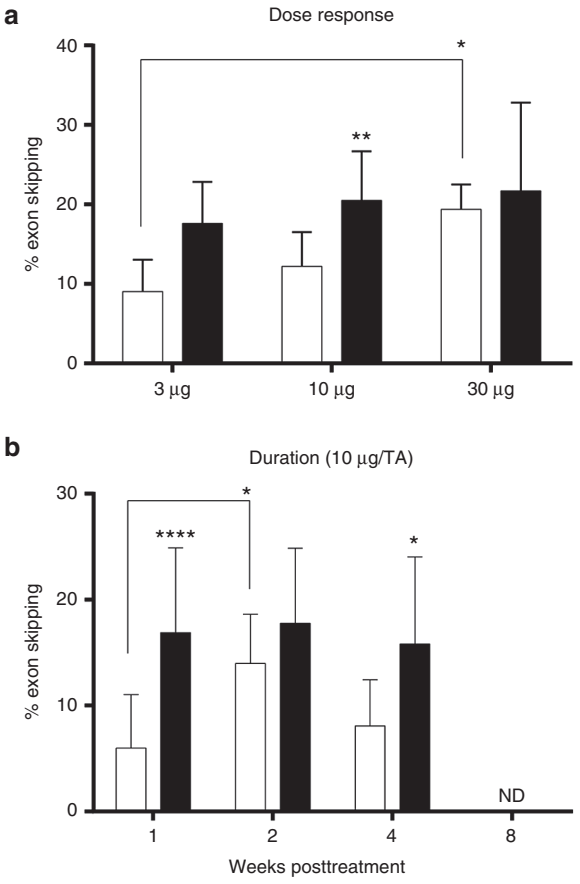

Figure 3 Dose response and duration of PNA activity of electrotransfer in NMRI mice. (**a**) Effect in TA muscles of increasing doses of PNA with or without electroporation (n = 6–14). (**b**) Duration of PNA after a single injection of 10 µg with or without electroporation (n = 14–15). Results are presented as mean + SD (white bars = injection, black = electroporation), not detectable (ND). Electroporation parameters: (8×175 V/cm, 20 ms, 1 Hz). Two-way ANOVA followed by Tukey multiple comparison test; *$P < 0.05$;**$P < 0.01$; ***$P < 0.0001$. ANOVA, analysis of variance; PNA, peptide nucleic acid; TA, tibialis anterior.

Duration of PNA electrotransfer in mdx mice

In order to examine the duration of exon skipping activity in mdx mice following a single-dose treatment, a time course study was performed (**Figure 6**). Analysis of whole muscle transverse sections showed recovery of dystrophin protein at the sarcolemma after 2, 4, and 8 weeks in PNA-treated muscles (**Figure 6a**), and a statistically significant overall enhancement by electroporation (two-way ANOVA, effect of electroporation, $P < 0.05$), and specifically statistical significance by the *post hoc* test was found at the 2 weeks time point ($P < 0.001$) (**Figure 6b** and **Supplementary Figure S3**). The latter finding was corroborated by RT-PCR determination of the PNA-induced dystrophin mRNA exon 23 skipping in the entire TA muscle (two-way ANOVA, effect of electroporation, $P < 0.01$) (**Figure 6d**). With PNA injection, only the average number of dystrophin-positive fibers was unchanged during the time course (~300 dystrophin-positive fibers,

Table 1 PNA oligomers

No.	Name	Sequence	Charge	Mass[a]	Purity
3684	Phophonate	H-(bisP4)$_4$-GGC CAA ACC TCG GCT TAC CT-NH2	–15	6794(6775)	95+ (b)
3687	R$_8$-deca	H-(D-Arg)$_8$-Lys(Deca)-GGC CAA ACC TCG GCT TAC CT-NH2	+9	6889(6890)	98+
3690	R$_8$	H-(D-Arg)$_8$-GGC CAA ACC TCG GCT TAC CT-NH2	+9	6610(6607)	98+
3696	Unmodified	H-GGC CAA ACC TCG GCT TAC CT-NH2	+1	5357(5358)	98+
4200	Mismatch	H-GGC CAA **C**CC TCG G**A**T TAC CT-NH2	+1	5358(5358)	98+
4258	(Lys)$_4$	H-(Lys)$_4$-GGC CAA ACC TCG GCT TAC CT-NH2	+5	5875(5871)	95+
4278	AF488	AF488-GGC CAA ACC TCG GCT TAC CT-NH2	–2	5879(5887)	98+

The sequences of the PNAs are written from the N-terminal to the C-terminal end. The mismatch bases are indicated in bold.
PNA, peptide nucleic acid.
[a]Mass (MW): found (calculated).

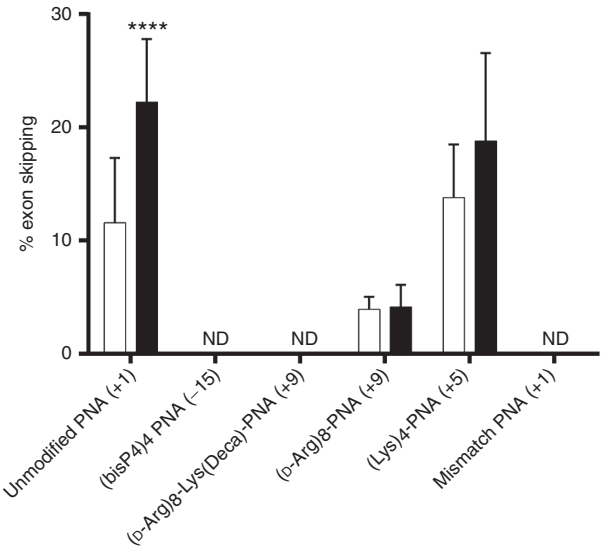

Figure 4 Electrotransfer of PNA conjugates with different charges in NMRI mice. PNA with the different modifications (see **Table 1** for abbreviations) were tested in combination with electroporation at 10 µg/TA (n = 4–7). Results are presented as mean + SD (white bars = injection, black = electroporation), not detectable (ND). Electroporation parameters: (8×175 V/cm, 20 ms, 1 Hz). Two-way ANOVA followed by Tukey multiple comparison test: ****P < 0.0001. ANOVA, analysis of variance; PNA, peptide nucleic acid; TA, tibialis anterior.

Supplementary Figure S3), whereas in the electroporated muscles, a decrease in the number of dystrophin-positive fibers from 2 to 8 weeks was indicated (from 851 (± 623) dystrophin-positive fibers at the 2-week time point dropping to 449 (±305) after 8 weeks (two-way ANOVA, effect of time, P < 0.0001) (**Figure 6b** and **Supplementary Figure S1c**). The number of dystrophin-positive fibers was higher in the proximal sections (two-way ANOVA, effect of location, P < 0.0001) as observed in the dose response in mdx mice. Hematoxylin and eosin staining of TA muscle sections from the time course study showed that the PNA treatment did not in this short period change the dystrophic pathology characterized by centrally nucleated fibers and fiber-size viability (**Figure 6c**). All muscles scored 3 in a visual analog scale for histopathology score[35] regardless of treatment (injection only or electroporation) and time (data not shown).

Electrotransfer of alexafluor488 (AF488) labelled PNA

To examine the distribution of injected PNA and whether the restoration of dystrophin-positive fibers was correlated to the PNA distribution, we used a 1:1 mixture AF488 fluorophore labeled (PNA 4278) and the unmodified PNA for injection at a final dose of 10 µg for each. Immunohistochemical evaluations revealed that dystrophin-positive fibers and PNA AF488 were largely located in the same areas of the muscle, but were clearly not totally colocalized (**Figure 7**). Fluorescent dots rather than a uniform staining were observed. As Alexa488 PNA has less water solubility than the unmodified PNA, we ascribe this behavior to aggregation of the labeled PNA in the tissue. We also note that most of the fluorescence is located outside the muscle fibers, reflecting the rather inefficient cellular uptake. Therefore, this experiment primarily confirms the conclusions drawn from sectional analysis of the muscle (**Figures 5c** and **6b**) that the PNA distribution within the muscle is quite uneven and that dystrophin activation overall parallels the PNA localization.

Discussion

In this study, we find that electroporation can augment PNA activity by twofold to fourfold in NMRI mice using a single PNA dose, and activity could be detected for up to 4 weeks at the RNA level. In dystrophic muscles, the effect of electroporation was less pronounced, but a significant increase in the number of dystrophin-positive fibers by 2.5-fold was demonstrated after 2 weeks from a single-dose administration.

In mdx mice, the muscle fiber uptake of AO is higher than that in normal mice due to the leaky membrane.[36,37] Thus, we ascribe the more pronounced electroporation enhancement observed in normal muscle versus dystrophic muscle tissue to the already compromised membrane in the dystrophic muscle, which may be relatively less affected by the application of an external electric field.

One other study has tested electroporation of an antisense oligonucleotide (2′-O-methyl phosphorothioate oligonucleotides (2′OMePS, charge-19)) in mdx mice using the same electric parameters as in this study, and ~3.5-fold enhancement in dystrophin-positive fibers 2 weeks after electrotransfer was reported.[26] In this study, hyaluronidase was used as a pretreatment to increase distribution in the muscle through degradation of hyaluronan, a component in the extracellular matrix, and hyaluronidase pretreatment has previously been shown to increase the effect of transfection efficiencies of DNA.[38,39] Thus, the *ca.* 2.5-fold increase in dystrophin-positive fibers after PNA electrotransfer in mdx mice found in this study is comparable to the efficacy enhancement obtained in the above-described electroporation study with 2′OMePS and hyaluronidase treatment. In this study, a maximum of *ca.* 20% exon skipping in combination with electroporation was reached, and this is comparable to the number obtained in a previous study that reported 427(±46) dystrophin-positive fibers counted in one section 2 weeks after a single i.m. injection of 10 µg unmodified PNA.[21] In line with this, we find 346 (±309) dystrophin fibers as the average for three locations in the muscle using the same injection dose and time point. It is important to note that the number of positive fibers varies 10-fold (*ca.* 100–1,000 positive fibers) at the three different sections along the length of the muscle, presumably reflecting quite uneven PNA distribution upon i.m. administration. Therefore, considering that the highest RT-PCR splice correction value of 20% was obtained as an average from the entire muscle, the maximum splice correction in the part of the muscle receiving the highest local PNA dose must be significantly higher and could approach 60% as judged from the average number of positive fibers (*ca.* 300) compared to the area with highest fiber count (*ca.* 1,000). As further evidence of uneven distribution of the PNA in the muscle, and consequently of the biological effects, the experiments using an AF488-labeled PNA clearly indicated an uneven distribution of this as well as an overlap of muscle areas exhibiting PNA fluorescence and dystrophin staining.

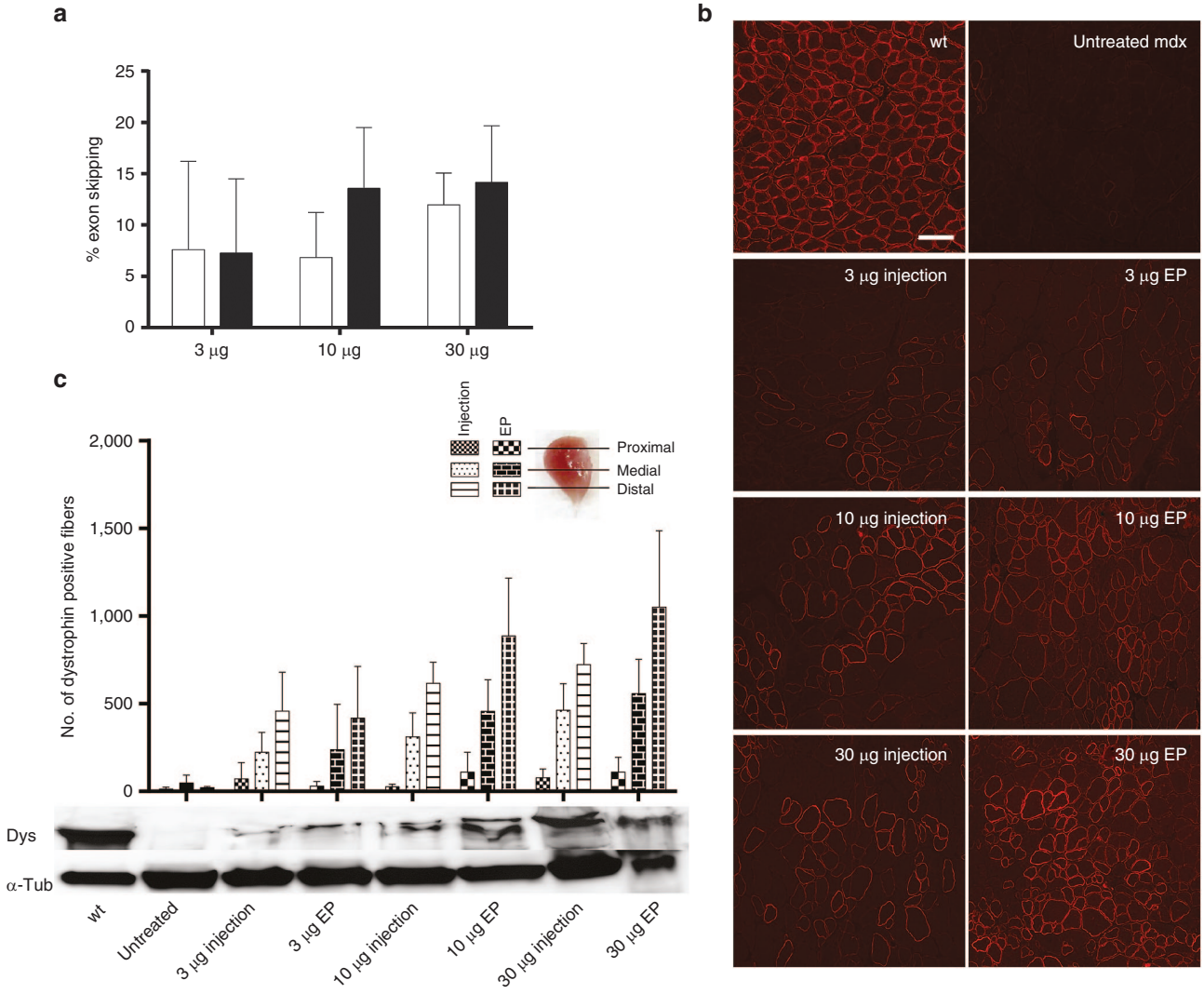

Figure 5 Electrotransfer of unmodified PNA in mdx mice. Effect of increasing doses of PNA in TA muscles with or without electroporation (8×175 V/cm, 20 ms, 1 Hz) analyzed 1 week after treatment (treated mdx: $n = 6–7$; control mdx: $n = 3$). (**a**) RT-PCR results are presented as mean+ SD (white bars = injection, black = electroporation). (**b**) Representative immunohistochemistry staining for dystrophin in TA muscles of mdx mice after i.m. injection of varying PNA concentrations plus/minus electroporation (bar = 50 μm). (**c**) Quantitative evaluation of total number of dystrophin-positive fibers in TA muscles after injection of varying PNA concentrations. The number of dystrophin-positive fibers is presented as mean + SD. The first bar of each group represents the distal section, the second bar the medial section, and the third bar the proximal section. Sections for immunohistochemistry were taken around the marked positions on the TA muscle, relative to the knee. Examples of western blot for treated muscles after injection of varying PNA dose with or without electroporation. Thirty-five micrograms of total muscle protein from a wt (c57BL10), untreated mdx, and PNA-treated mdx TA muscles was loaded. α-Tubulin was used as a loading control. EP, electroporation; PNA, peptide nucleic acid; TA, tibialis anterior.

Previous studies have reported time courses of the duration of single i.m. administration of analogous phosphorothioate oligonucleotides, phosphoamidate morpholino, or PNA derivatives comparable to the ones found in this study.[26,40,41]

The increased number of dystrophin-positive fibers at 2 weeks after injection with or without electroporation is consistent with the increased level of exon 23 skipped dystrophin RNA, while several factors are likely to contribute to the time course of dystrophin-positive fiber decline after 2 weeks. These include half-life of PNA in the muscle cells, half-life of dystrophin mRNA and protein, as well as the relentlessly ongoing degeneration–regeneration cycle. As many dystrophin-positive fibers were small, newly formed fibers, the dystrophin level at the membrane in these fibers may be too low to detect once the fibers are reaching mature size. Additionally, even as newly formed fibers enjoy added protection in the form of an increased level of a number of membrane proteins like utrophin and alpha7-integrin,[42–44] this effect will have tapered off at 3–4 weeks after formation, leaving the fiber vulnerable to degeneration. Obviously, vulnerability to degeneration will depend on the initial PNA-mediated level of dystrophin as well as distribution. As a high local level dystrophin is probably less efficient in attenuating the wear and tear of the fibers, it may even increase the degeneration due to an uneven stress on the muscle fibers, compared to a more widespread but lower per-fiber concentration of dystrophin.

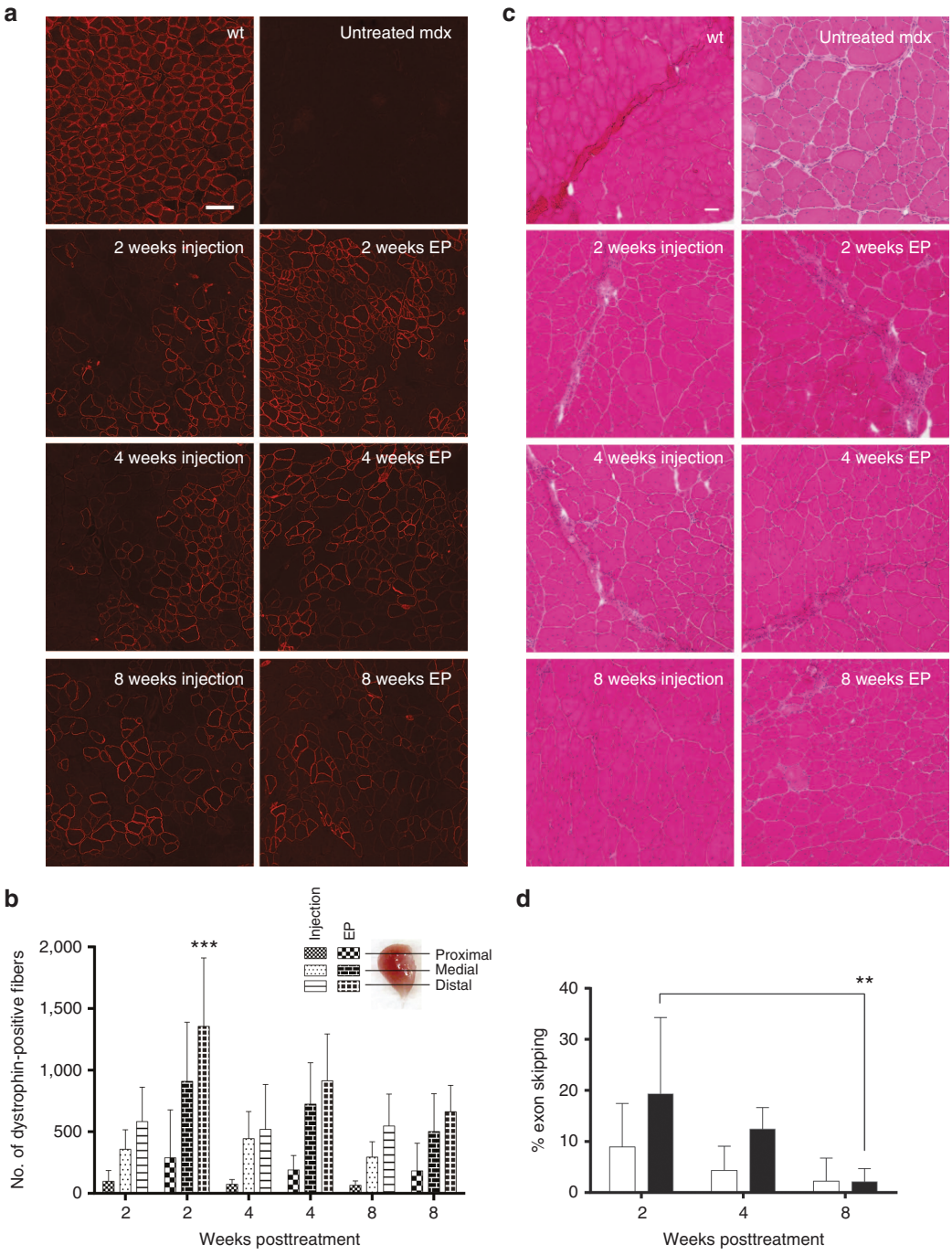

Figure 6 Duration of PNA effect in mdx mice (10 µg/TA). (**a**) Dystrophin expression detected by immunohistochemistry staining at different time points after a single injection of 10 µg PNA with or without electroporation (8×175 V/cm, 20 ms, 1 Hz) in mdx mice (bar = 50 µm). (**b**) Total number of dystrophin-positive fibers at different time points with or without electroporation (n = 6–8). Data are presented as mean + SD. The first bar of each group represents the distal section, the second bar the medial section, and the third bar the proximal section. Sections for histology and immunohistochemistry were taken around the marked positions on the TA muscle, relative to the knee. Two-way ANOVA followed by Tukey multiple comparison test: ***P < 0.001. (**c**) Hematoxylin and eosin staining of wt and mdx TA muscles at different time points after a single injection with or without electroporation (bar = 50 µm). (**d**) Duration of PNA effect measured by exon skipping. Results are presented as mean + SD (white bars = injection, black = electroporation). Two-way ANOVA followed by Tukey multiple comparison test: **P < 0.01. EP, electroporation. ANOVA, analysis of variance; PNA, peptide nucleic acid; TA, tibialis anterior.

It is somewhat surprising that LV pulses, which are also preferred for polycationic oligonucleotides (and also DNA vectors), were the most efficient for electroporation delivery of the charge neutral PNA to the muscle. Perhaps even more unexpectedly, PNA efficiency was not improved by using neither anionic nor cationic PNA derivatives. In particular, improved activity could have been anticipated with the anionic oligophosphonate ligand, which in the pLuc Hela

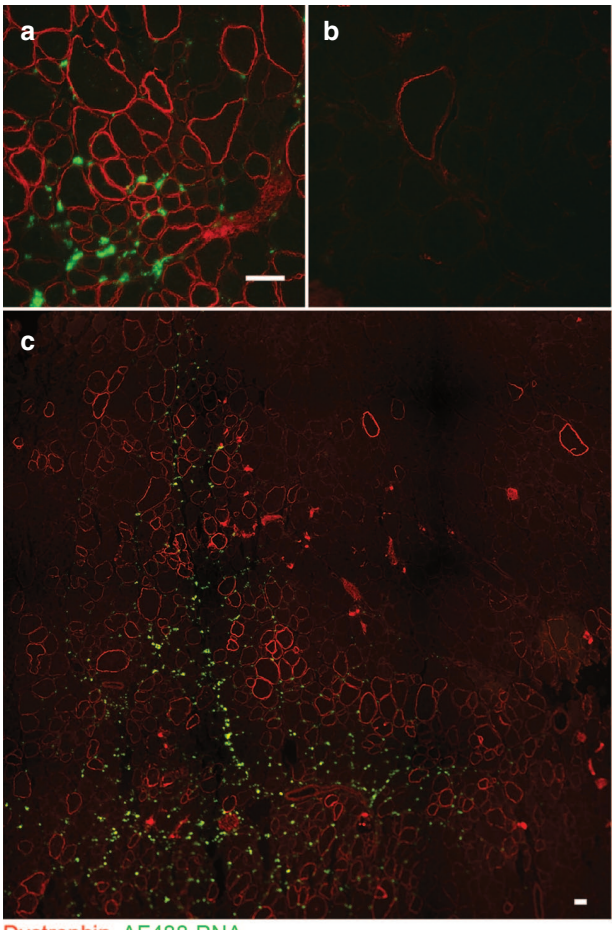

Figure 7 Electroporation of Alexa fluor 488–labeled PNA. Immunohistochemical staining of dystrophin expression in mdx TA muscles following injection and electroporation of 10 µg PNA 3696 (unmodified) +10 µg PNA 4278, 1 week posttreatment (bar = 50 µm). (**a**) Image from injected area, (**b**) image from uninjected region, and (**c**) a broader section of a muscle cross-section. PNA, peptide nucleic acid; TA, tibialis anterior.

cell luciferase splice redirection model system has exhibited extremely high potency when delivered via cationic lipids,[45] and for which, like ordinary oligonucleotides, electroporation delivery could be aided by electric field–dependent migration of the PNA. Thus, we can offer no simple explanation at this stage for the structure–activity relations seen in this study, and they are most likely the results of multitude of factors including limited diffusion in the muscle tissue due to binding to extracellular matrix and cell surface in combination with differences in response to the electroporation process.

In conclusion, we have shown that electroporation can augment antisense activity of unmodified PNA at low doses by twofold to fourfold in healthy mice muscle after i.m. administration, while an enhancement of the number of dystrophin-positive fibers of up to 2.5-fold was seen in dystrophic muscles in MDX mouse 2 weeks after treatment. Clinical use of antisense therapy for treatment of DMD patients requires systemic administration of the drug because all muscles including heart muscle are affected by the disease and must be treated. Thus, although the present data show some added benefit of electroporation in dystrophic muscle, further studies on systemically administered modified PNAs are needed to elucidate if electroporation could eventually provide therapeutic enhancement in selected muscles. Indeed in DMD patients, upper extremity muscles, especially finger flexors may well benefit from local antisense treatment to extent patients abilities to control a motorized wheelchair joystick. Finally, other possible future indications based on PNA administration to muscle tissue may benefit from including an electroporation strategy.

Materials and methods

Animals. All animal experiments were conducted in accordance with the recommendations of the European Convention for the Protection of Vertebrate Animals used for Experimentation and after permission from the Danish Animal Experiments Inspectorate. Female NMRI mice at 11–13 weeks of age (bred at animal facility at Copenhagen University Hospital Herlev, Denmark, FELASA tested) and female and male mdx mice 11–13 weeks of age (bred at the animal facility at Panum Institue, University of Copenhagen, Denmark) were used in the experiments. The mice were randomly assigned to the different experimental groups (n = 4–15). The mice were maintained in a thermostated environment at a 12:12-hour light–dark cycle and had access to a rodent chow diet and water *ad libitum*. Mice were euthanized by quick cervical dislocation after 7 days (unless otherwise stated), and the TA muscles were excised and either snap-frozen in liquid nitrogen–cooled isopentane and stored at –80 °C or placed in RNA*later* (Ambion, Thermo Fisher Scientific, Waltham, MA) and stored at 4 °C.

PNA synthesis. Details of PNA and PNA conjugates are shown in **Table 1**. All the PNAs have the same base sequence directed against the 5′ (donor) splice site of intron 23 (M23D (+02-18)) in the murine DMD gene, which previously has been shown to induce exon 23 skipping.[21,22,41] PNA synthesis was carried out by the *tBoc* method as described previously.[33,45,46]

In vivo PNA electrotransfer. NMRI mice were anesthetized by i.p. injection of Hypnorm (Nomeco A/S, Copenhagen, Denmark) and midazolam (Hameln Pharmaceuticals, Hameln, Germany) and the mdx strain by inhalation of isoflurane (Baxter, Deerfield, IL) (4–5% isoflurane for induction and 2–3% for maintenance with 180 ml/minute oxygen). Solution of 10–40 µl containing 3–30 µg PNA (diluted in either saline or isotonic glucose) was injected i.m. into TA muscles along the fiber orientation using an insulin syringe. PNA concentration was calculated on the basis of molar concentration measured spectrophotometrically and using the molecular weight of the PNA. This was done due to variable salt content in the PNA preparations. *Ca.* 30 seconds later, plate electrodes (IGEA, Carpi, Italy) with either 4 or 5 mm gap (for NMRI or mdx mice, respectively) were fitted around the hind legs. To ensure good contact between the electrode and the skin, hair was removed, and electrode gel (EKO-GEL, Holstebro, Denmark) was applied. The electric field was delivered using a square wave generator (Cliniporator; IGEA). The following pulse

parameters were tested: 8 pulses at 1 Hz of: (100 µs, 600, 800, and 1,000 V/cm (applied voltage to electrode distance)) (HV), (20 ms, 125, 150, 175, 200, 225, and 250 V/cm) (LV), and a combination of 1 HV and 1 LV pulse (1 × 800 V/cm, 100 µs + 1 × 80 V/cm, 400 ms) (HVLV).

RNA extraction and RT-PCR. Total RNA was isolated from TA muscles by tissue homogenization and RNA extraction using the TRIzol reagent (Ambion, Thermo Fisher Scientific). cDNA was generated using 150 ng of total RNA and qScribt reverse transcriptase (RT) (Quanta Biosciences, Gaithersburg, MD) with a blend of random and oligo dT primers according to the manufacturer's instructions. Subsequently, 2 µl cDNA was used for each PCR with Brilliant II SYBR Green (Agilent, Santa Clara, CA) in 25 µl. The primers used were forward 5′-atccagcagtcagaaagcaaa-3′ (m22f) and reverse 5′-cag ccatccatttctgtaagg-3′ (m24r).[47] The PCR program was as follows: (95 °C, 10 minutes) × 1 cycle, (95 °C, 30 seconds; 60 °C, 30 seconds; 72 °C, 45 seconds) × 33 cycles, and (95 °C, 1 minutes; 60 °C, 30 seconds; 95 °C, 30 seconds) × 1 cycle. The products were analyzed on a 1.5% agarose gel with 1× TBE buffer and stained with ethidium bromide. Gel images were captured by ImageMaster (Syngene, Cambrigde, UK) and analyzed by UN-SCAN-IT software (Silk Scientific Corporation Silk Scientific, Orem, UT) to determine exon skipping percentage.

Immunohistochemistry and histology. Frozen, serial sections of 10 µm were cut for histology and immunohistology at three positions along each TA muscle (**Figure 5c**). The first sections were used for determination of dystrophin expression, and the second sections were used for hematoxylin and eosin staining. To examine overall muscle morphology and assess the level of infiltrating mononuclear cells, a 3-point visual analog score was used as described previously by Krag *et al.*[48] The intervening sections were collected for RT-PCR and western blotting. Determination of dystrophin expression was evaluated at three equidistant points along the muscle (proximal, medial, and distal relative to the knee). For dystrophin and laminin visualization and quantification, the first sections were blocked in buffer (3% fetal calf serum in phosphate-buffered saline) prior to staining. Primary antibodies, antidystrophin (ab15277; Abcam, Cambridge, UK) and anti-laminin-2 merosin (Clone 4H8-2; Sigma-Aldrich, St Louis, MO) were diluted 1:500 and incubated overnight at 4 °C. Alexa Fluor 594 antirabbit and Alexa Flour 488 antirat secondary antibodies (Life Technologies, Grand Island, NY) were used at a 1:500 dilution and incubated for 1 hour at room temperature. A Nikon 80i epi-fluorescence microscope with motorized x/y table and a Nikon DS-Ri1 camera (Nikon, Tokyo, Japan) was used to take pictures of the entire section. The number of dystrophin-positive fibers in the merged pictures of each stained cryosection was counted using Adobe Photoshop CS5 Extended. The person was blinded with regard to dose and treatment during counting.

Protein extraction and western blotting. Sections from TA muscles were homogenized in ice-cold lysis buffer with protease and phosphatase inhibitors (10 mmol/l Tris, pH7.4, 0.1% Triton-X 100, 0.5% sodium deoxycholate, 0.07 U/ml aprotinin, 20 µmol/l leupeptin, 20 µmol/l pepstatin, 1 mmol/l phenylmethanesulfonyl fluoride, 1 mmol/l ethylenediaminetetraacetic acid, 1 mmol/l (ethylene glycol tetraacetic acid, 1 mmol/l dithiothreitol) using a bead-mill at 4 °C. Supernatants were collected and protein concentrations were determined using the Bradford assay. Equal amounts of extracted muscle proteins were separated on 10% TGX polyacrylamide gels (Bio-Rad, Hercules, CA) at 200 V for 30 minutes. Proteins were transferred to polyvinylidene fluoride membranes, which were blocked in Baileys Irish Cream (Dublin, Ireland) for 30 minutes and incubated overnight with dystrophin antibody (ab15277; Abcam, Cambridge, UK). Secondary antibody coupled with horseradish peroxidase diluted 1:10,000 were used to detect primary antibodies (DAKO, Glostrup, Denmark). Immunoreactive bands were detected using a SuperSignal West Dura kit (ThermoFisher Scientific, Waltham, MA) and visualized using a GBox XT16 darkroom (Syngene, Cambridge, UK).

Statistical analysis. All data are reported as means ± SD. GraphPad Prism 6 (GraphPad Software, La Jolla, CA) was used for statistical analyses. To assess the efficacy of different electric pulse parameters (LV, HV, and HVLV) on PNA uptake (activity) (**Figure 1a**), a Student's *t*-test was performed. For assessment of the effect of LV pulses on PNA activity, a one-way ANOVA followed by *post hoc* Dunnetts multiple comparisons test was performed. For assessment of the effect of treatment groups (injection versus electroporation) and different volumes, doses, and time points (**Figures 2–6** and **Supplementary Figures S1–S3**), two-way ANOVA followed by *post hoc* Tukey multiple comparison test was performed. *P* values below 0.05 were considered statistically significant.

Supplementary material

Figure S1. Injection volume and dose response in NMRI mice.
Figure S2. Dose response study in mdx mice.
Figure S3. Duration study in mdx mice.

Acknowledgments. The authors thank Marianne Fregil, Birgit Hertz, Lone Christiansen, Anne Boye and Thomas Lauridsen for their technical assistance, and Jolanta Ludvigsen for PNA synthesis. Julie Gehl was a Royal Academy Research Fellow supported by the Acta Oncologica Foundation. The authors declare no conflict of interest.

1. Nielsen, PE (2010). Gene targeting and expression modulation by peptide nucleic acids (PNA). *Curr Pharm Des* **16**: 3118–3123.
2. Ganguly, S, Chaubey, B, Tripathi, S, Upadhyay, A, Neti, PV, Howell, RW *et al.* (2008). Pharmacokinetic analysis of polyamide nucleic-acid-cell penetrating peptide conjugates targeted against HIV-1 transactivation response element. *Oligonucleotides* **18**: 277–286.
3. Sazani, P, Gemignani, F, Kang, SH, Maier, MA, Manoharan, M, Persmark, M *et al.* (2002). Systemically delivered antisense oligomers upregulate gene expression in mouse tissues. *Nat Biotechnol* **20**: 1228–1233.
4. Nielsen, PE (2004). PNA technology. *Mol Biotechnol* **26**: 233–248.
5. Wancewicz, EV, Maier, MA, Siwkowski, AM, Albertshofer, K, Winger, TM, Berdeja, A *et al.* (2010). Peptide nucleic acids conjugated to short basic peptides show improved pharmacokinetics and antisense activity in adipose tissue. *J Med Chem* **53**: 3919–3926.
6. Marty, M, Sersa, G, Garbay, JR, Gehl, J, Collins, CG, Snoj, M *et al.* (2006). Electrochemotherapy - an easy, highly effective and safe treatment of cutaneous and subcutaneous metastases: results of ESOPE (European Standard Operating Procedures of Electrochemotherapy) study. *Ejc Suppl* **4**: 3–13.
7. Mir, LM, Gehl, J, Sersa, G, Collins, CG, Garbay, JR, Billard, V *et al.* (2006). Standard operating procedures of the electrochemotherapy: instructions for the use of bleomycin

or cisplatin administered either systemically or locally and electric pulses delivered by the Cliniporator (TM) by means of invasive or non-invasive electrodes. *Ejc Suppl* **4**: 14–25.
8. Agerholm-Larsen, B, Iversen, HK, Ibsen, P, Moller, JM, Mahmood, F, Jensen, KS *et al.* (2011). Preclinical validation of electrochemotherapy as an effective treatment for brain tumors. *Cancer Res* **71**: 3753–3762.
9. Miklavčič, D, Serša, G, Brecelj, E, Gehl, J, Soden, D, Bianchi, G *et al.* (2012). Electrochemotherapy: technological advancements for efficient electroporation-based treatment of internal tumors. *Med Biol Eng Comput* **50**: 1213–1225.
10. Frandsen, SK, Gissel, H, Hojman, P, Tramm, T, Eriksen, J and Gehl, J (2012). Direct therapeutic applications of calcium electroporation to effectively induce tumor necrosis. *Cancer Res* **72**: 1336–1341.
11. Matthiessen, LW, Chalmers, RL, Sainsbury, DC, Veeramani, S, Kessell, G, Humphreys, AC *et al.* (2011). Management of cutaneous metastases using electrochemotherapy. *Acta Oncol* **50**: 621–629.
12. Rosazza, C, Buntz, A, Rieß, T, Wöll, D, Zumbusch, A and Rols, MP (2013). Intracellular tracking of single-plasmid DNA particles after delivery by electroporation. *Mol Ther* **21**: 2217–2226.
13. Markelc, B, Skvarca, E, Dolinsek, T, Kloboves, VP, Coer, A, Sersa, G *et al.* (2015). Inhibitor of endocytosis impairs gene electrotransfer to mouse muscle in vivo. *Bioelectrochemistry* **103**: 111–119.
14. Joergensen, M, Agerholm-Larsen, B, Nielsen, PE and Gehl, J (2011). Efficiency of cellular delivery of antisense peptide nucleic acid by electroporation depends on charge and electroporation geometry. *Oligonucleotides* **21**: 29–37.
15. Brolin, C and Shiraishi, T (2011). Antisense mediated exon skipping therapy for duchenne muscular dystrophy (DMD). *Artif DNA PNA XNA* **2**: 6–15.
16. van Deutekom, JC, Janson, AA, Ginjaar, IB, Frankhuizen, WS, Aartsma-Rus, A, Bremmer-Bout, M *et al.* (2007). Local dystrophin restoration with antisense oligonucleotide PRO051. *N Engl J Med* **357**: 2677–2686.
17. Kinali, M, Arechavala-Gomeza, V, Feng, L, Cirak, S, Hunt, D, Adkin, C *et al.* (2009). Local restoration of dystrophin expression with the morpholino oligomer AVI-4658 in Duchenne muscular dystrophy: a single-blind, placebo-controlled, dose-escalation, proof-of-concept study. *Lancet Neurol* **8**: 918–928.
18. Voit, T, Topaloglu, H, Straub, V, Muntoni, F, Deconinck, N, Campion, G *et al.* (2014). Safety and efficacy of drisapersen for the treatment of Duchenne muscular dystrophy (DEMAND II): an exploratory, randomised, placebo-controlled phase 2 study. *Lancet Neurol* **13**: 987–996.
19. Lu, QL, Cirak, S and Partridge, T (2014). What can we learn from clinical trials of exon skipping for DMD? *Mol Ther Nucleic Acids* **3**: e152.
20. Mendell, JR, Rodino-Klapac, LR, Sahenk, Z, Roush, K, Bird, L, Lowes, LP *et al.*; Eteplirsen Study Group. (2013). Eteplirsen for the treatment of Duchenne muscular dystrophy. *Ann Neurol* **74**: 637–647.
21. Yin, H, Lu, Q and Wood, M (2008). Effective exon skipping and restoration of dystrophin expression by peptide nucleic acid antisense oligonucleotides in mdx mice. *Mol Ther* **16**: 38–45.
22. Ivanova, GD, Arzumanov, A, Abes, R, Yin, H, Wood, MJ, Lebleu, B *et al.* (2008). Improved cell-penetrating peptide-PNA conjugates for splicing redirection in HeLa cells and exon skipping in mdx mouse muscle. *Nucleic Acids Res* **36**: 6418–6428.
23. Kishida, T, Asada, H, Gojo, S, Ohashi, S, Shin-Ya, M, Yasutomi, K *et al.* (2004). Sequence-specific gene silencing in murine muscle induced by electroporation-mediated transfer of short interfering RNA. *J Gene Med* **6**: 105–110.
24. Golzio, M, Mazzolini, L, Moller, P, Rols, MP and Teissié, J (2005). Inhibition of gene expression in mice muscle by *in vivo* electrically mediated siRNA delivery. *Gene Ther* **12**: 246–251.
25. Faria, M, Spiller, DG, Dubertret, C, Nelson, JS, White, MR, Scherman, D *et al.* (2001). Phosphoramidate oligonucleotides as potent antisense molecules in cells and *in vivo*. *Nat Biotechnol* **19**: 40–44.
26. Wells, KE, Fletcher, S, Mann, CJ, Wilton, SD and Wells, DJ (2003). Enhanced *in vivo* delivery of antisense oligonucleotides to restore dystrophin expression in adult mdx mouse muscle. *FEBS Lett* **552**: 145–149.
27. Hojman, P, Gissel, H, Andre, FM, Cournil-Henrionnet, C, Eriksen, J, Gehl, J *et al.* (2008). Physiological effects of high- and low-voltage pulse combinations for gene electrotransfer in muscle. *Hum Gene Ther* **19**: 1249–1260.
28. Wang, XD, Tang, JG, Xie, XL, Yang, JC, Li, S, Ji, JG *et al.* (2005). A comprehensive study of optimal conditions for naked plasmid DNA transfer into skeletal muscle by electroporation. *J Gene Med* **7**: 1235–1245.
29. Hartikka, J, Sukhu, L, Buchner, C, Hazard, D, Bozoukova, V, Margalith, M *et al.* (2001). Electroporation-facilitated delivery of plasmid DNA in skeletal muscle: plasmid dependence of muscle damage and effect of poloxamer 188. *Mol Ther* **4**: 407–415.
30. Tennyson, CN, Shi, Q and Worton, RG (1996). Stability of the human dystrophin transcript in muscle. *Nucleic Acids Res* **24**: 3059–3064.
31. Wu, B, Lu, P, Cloer, C, Shaban, M, Grewal, S, Milazi, S *et al.* (2012). Long-term rescue of dystrophin expression and improvement in muscle pathology and function in dystrophic mdx mice by peptide-conjugated morpholino. *Am J Pathol* **181**: 392–400.
32. Verhaart, IE, van Vliet-van den Dool, L, Sipkens, JA, de Kimpe, SJ, Kolfschoten, IG, van Deutekom, JC *et al.* (2014). The dynamics of compound, transcript, and protein effects after treatment with 2OMePS antisense oligonucleotides in mdx mice. *Mol Ther Nucleic Acids* **3**: e148.
33. Koppelhus, U, Shiraishi, T, Zachar, V, Pankratova, S and Nielsen, PE (2008). Improved cellular activity of antisense peptide nucleic acids by conjugation to a cationic peptide-lipid (CatLip) domain. *Bioconjug Chem* **19**: 1526–1534.
34. Shiraishi, T, Hamzavi, R and Nielsen, PE (2008). Subnanomolar antisense activity of phosphonate-peptide nucleic acid (PNA) conjugates delivered by cationic lipids to HeLa cells. *Nucleic Acids Res* **36**: 4424–4432.
35. Hauerslev, S, Sveen, ML, Duno, M, Angelini, C, Vissing, J and Krag, TO (2012). Calpain 3 is important for muscle regeneration: evidence from patients with limb girdle muscular dystrophies. *BMC Musculoskelet Disord* **13**: 43.
36. Matsuda, R, Nishikawa, A and Tanaka, H (1995). Visualization of dystrophic muscle fibers in mdx mouse by vital staining with Evans blue: evidence of apoptosis in dystrophin-deficient muscle. *J Biochem* **118**: 959–964.
37. Heemskerk, HA, de Winter, CL, de Kimpe, SJ, van Kuik-Romeijn, P, Heuvelmans, N, Platenburg, GJ *et al.* (2009). *In vivo* comparison of 2'-O-methyl phosphorothioate and morpholino antisense oligonucleotides for Duchenne muscular dystrophy exon skipping. *J Gene Med* **11**: 257–266.
38. McMahon, JM, Signori, E, Wells, KE, Fazio, VM and Wells, DJ (2001). Optimisation of electrotransfer of plasmid into skeletal muscle by pretreatment with hyaluronidase – increased expression with reduced muscle damage. *Gene Ther* **8**: 1264–1270.
39. Mennuni, C, Calvaruso, F, Zampaglione, I, Rizzuto, G, Rinaudo, D, Dammassa, E *et al.* (2002). Hyaluronidase increases electrogene transfer efficiency in skeletal muscle. *Hum Gene Ther* **13**: 355–365.
40. Lu, QL, Mann, CJ, Lou, F, Bou-Gharios, G, Morris, GE, Xue, SA *et al.* (2003). Functional amounts of dystrophin produced by skipping the mutated exon in the mdx dystrophic mouse. *Nat Med* **9**: 1009–1014.
41. Yin, H, Betts, C, Saleh, AF, Ivanova, GD, Lee, H, Seow, Y *et al.* (2010). Optimization of peptide nucleic acid antisense oligonucleotides for local and systemic dystrophin splice correction in the mdx mouse. *Mol Ther* **18**: 819–827.
42. Hodges, BL, Hayashi, YK, Nonaka, I, Wang, W, Arahata, K and Kaufman, SJ (1997). Altered expression of the alpha7beta1 integrin in human and murine muscular dystrophies. *J Cell Sci* **110**: 2873–2881.
43. Helliwell, TR, Man, NT, Morris, GE and Davies, KE (1992). The dystrophin-related protein, utrophin, is expressed on the sarcolemma of regenerating human skeletal muscle fibres in dystrophies and inflammatory myopathies. *Neuromuscul Disord* **2**: 177–184.
44. Zhao, J, Yoshioka, K, Miike, T and Miyatake, M (1993). Developmental studies of dystrophin-positive fibers in mdx, and DRP localization. *J Neurol Sci* **114**: 104–108.
45. Shiraishi, T and Nielsen, PE (2012). Nanomolar cellular antisense activity of peptide nucleic acid (PNA) cholic acid ("umbrella") and cholesterol conjugates delivered by cationic lipids. *Bioconjug Chem* **23**: 196–202.
46. Christensen, L, Fitzpatrick, R, Gildea, B, Petersen, KH, Hansen, HF, Koch, T *et al.* (1995). Solid-phase synthesis of peptide nucleic acids. *J Pept Sci* **1**: 175–183.
47. Spitali, P, Heemskerk, H, Vossen, RH, Ferlini, A, den Dunnen, JT, 't Hoen, PA *et al.* (2010). Accurate quantification of dystrophin mRNA and exon skipping levels in duchenne muscular dystrophy. *Lab Invest* **90**: 1396–1402.
48. Krag, TO, Hauerslev, S, Sveen, ML, Schwartz, M and Vissing, J (2011). Level of muscle regeneration in limb-girdle muscular dystrophy type 2I relates to genotype and clinical severity. *Skelet Muscle* **1**: 31.

Supplementary Information accompanies this paper on the Molecular Therapy–Nucleic Acids website (http://www.nature.com/mtna)